Dislocation Profiles in HgCdTe(100) on GaAs(100) Grown by Metalorganic Chemical Vapor Deposition

H. NISHINO, S. MURAKAMI, T. SAITO, Y. NISHIJIMA, and H. TAKIGAWA

Fujitsu Laboratories Ltd., 10-1 Morinosato-Wakamiya, Atsugi 243-01, Japan

We studied dislocation etch pit density (EPD) profiles in HgCdTe(100) layers grown on GaAs(100) by metalorganic chemical vapor deposition. Dislocation profiles in HgCdTe(111)B and HgCdTe(100) layers differ as follows: Misfit dislocations in HgCdTe(111)B layers are concentrated near the HgCdTe/CdTe interfaces because of slip planes parallel to the interfaces. Away from the HgCdTe/CdTe interface, the HgCdTe(111)B dislocation density remains almost constant. In HgCdTe(100) layers, however, the dislocations propagate monotonically to the surface and the dislocation density decreases gradually as dislocations are incorporated with increasing HgCdTe(100) layer thicknesses. The dislocation reduction was small in HgCdTe(100) layers more than 10 μm from the HgCdTe/CdTe interface. The CdTe(100) buffer thickness and dislocation density were similarly related. Since dislocations glide to accommodate the lattice distortion and this movement increases the probability of dislocation incorporation, incorporation proceeds in limited regions from each interface where the lattice distortion and strain are sufficient. We obtained the minimum EPD in HgCdTe(100) of 1 to 3×10^6 cm^{-2} by growing both the epitaxial layers more than 8 μm thick.

Key words: CdTe buffer, dislocation, etch pit density (EPD), HgCdTe, incorporation of dislocations, lattice mismatch strain, metalorganic chemical vapor deposition (MOCVD), slip plane

INTRODUCTION

Heteroepitaxial growth of CdTe or HgCdTe on GaAs has been studied tor use in fabricating large-area infrared focal plane arrays. Metalorganic chemical vapor deposition (MOCVD) is one of the most promising techniques for growing HgCdTe, because of its high throughput and suitability for large-area substrates.

Direct alloy growth (DAG)[1,2] and the interdiffused multilayer process (IMP)[3,4] were developed to prepare HgCdTe layers by MOCVD. In DAG, an epitaxial layer of the alloy is grown by supplying all the sources simultaneously. In IMP, thin epitaxial layers of CdTe and HgTe are grown alternately and interdiffused completely to form the alloy by annealing. Direct alloy growth produces a poorer compositional uniformity than IMP[5,6] because of the very different formation energies of CdTe and HgTe. But recent advances such as using a multinozzle injector[7] or a wide reaction cell[8] can solve this problem. Historically, DAG has been expected to produce a lower dislocation density than IMP[8] because the IMP layers contain many interfaces with growth interruptions which increase misfit dislocations.

Metalorganic chemical vapor deposition forms both HgCdTe(100)[2,9] and HgCdTe(111)B[10,11] epitaxial layers on GaAs(100) substrates because of the large lattice mismatch (14.6%) between GaAs and CdTe buffer layers. HgCdTe(100) layers have a higher arsenic doping efficiency than HgCdTe(111)B layers.[12] Since arsenic is a commonly used acceptor which diffuses slowly in HgCdTe[13] and donor doping is easy for both orientations,[14,15] HgCdTe(100) is an attractive plane for constructing abrupt pn junctions for infrared photodiodes.

High-quality long-wavelength infrared detectors require HgCdTe(100) layers with a low dislocation

(Received October 13, 1993; revised September 13, 1994)

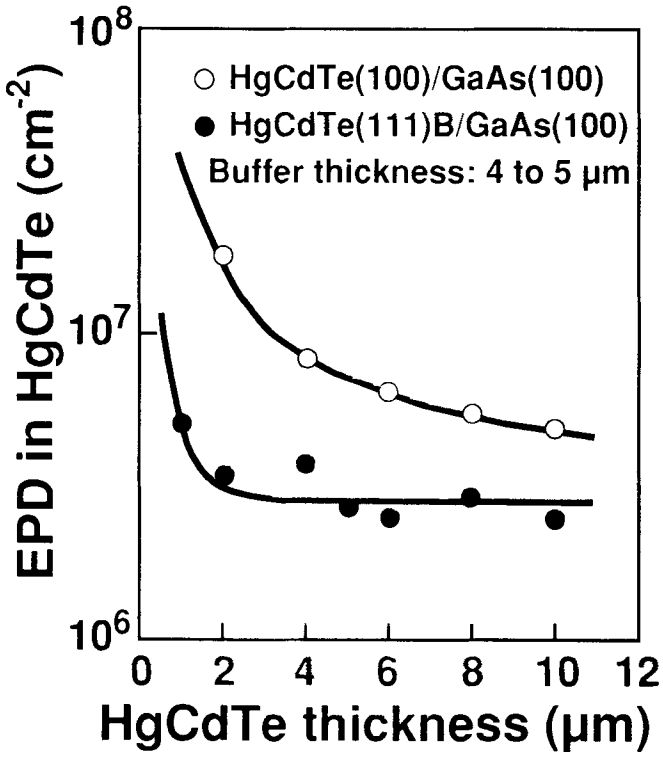

Fig. 1. Etch pit density thickness profiles in HgCdTe(111)B and HgCdTe(100) layers CdTe buffer thickness for both layers is 4 to 5 μm.

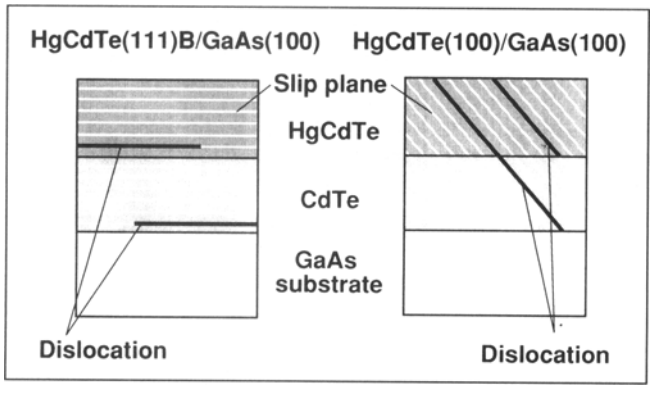

Fig. 2. Propagation of misfit dislocations in HgCdTe/CdTe/GaAs(100) with two epitaxial orientations (111)B and (100). Dislocations are generated at each interface and propagate along {111} slip planes.

density,[16] but the dislocation density in HgCdTe layers grown on GaAs substrates is high because of the large lattice mismatch. Dislocations in HgCdTe(111)B on CdZnTe(111)B grown by liquid phase epitaxy (LPE) have been well studied[17,18] but, to our knowledge a study of MOCVD-grown HgCdTe layers has not been published. We studied the dislocation profiles in HgCdTe(100) on GaAs(100) grown by MOCVD (DAG). We considered the dependence of the dislocation density on the thickness of both the HgCdTe and CdTe buffer layers and the dislocation reduction mechanism in these layers.

EXPERIMENTAL

We did the epitaxial growth in a horizontal reactor with multiple nozzles and a rotatiing graphite susceptor heated by radio frequency induction.[19] We

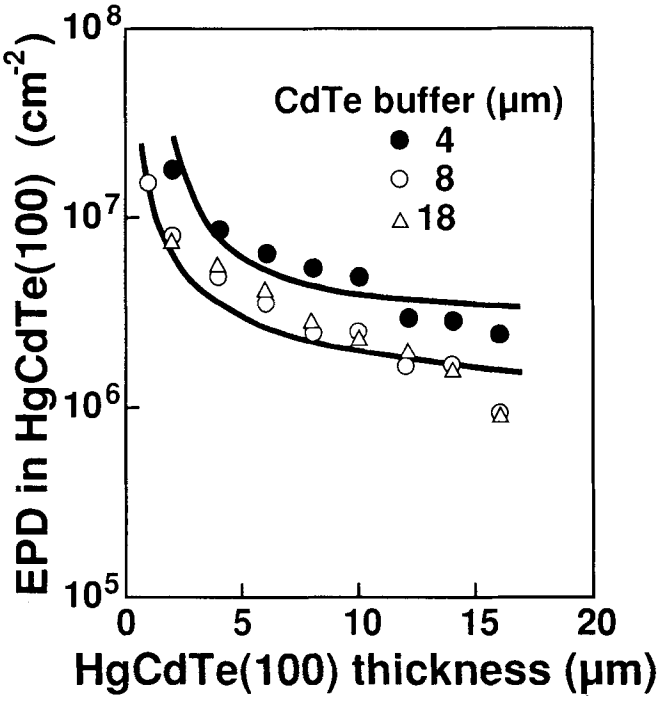

Fig. 3. Etch pit density thickness profiles in HgCdTe(100) layers grown on different thick CdTe(100) buffer layers.

used 3 inch GaAs substrates (100) misoriented 2° toward the nearest (110). To improve the compositional uniformity, we simultaneously injected the three precursors, dimethylcadmium (DMCd), diisopropyltelluride (DIPTe), and elemental mercury (Hg) into the reactor from different nozzles.

We preheated the GaAs substrates at 600°C for 20 min and grew the CdTe buffer layers at 410°C under low pressure (150 Torr) to improve thickness uniformity. Since we grew both (100) and (111)B oriented layers to compare dislocation profiles, before buffer growth, we treated the substrates as follows. To obtain the CdTe(111)B layer, we first introduced DIPTe into the reactor at 410°C, which formed a relatively Te-poor Ga-As-Te interfacial phase and caused (111)B growth.[20,21] To form the CdTe(100) layer, we supplied DMCd and DIPTe simultaneously. We also deposited the CdTe buffer layers for each orientation under different VI/II source gas ratios and growth rates a relatively high VI/II ratio[22] and a growth rate of 2 μm/h for the (111)B layer and a relatively low VI/II ratio[23] and a growth rate of 3 μm/h for the (100) layer.

We grew the HgCdTe layers at 360°C under atmospheric pressure. After growing the CdTe(100) buffers, we cleaved the substrates into small pieces and loaded several samples with different buffer thicknesses (4 to 18 μm) together into the reactor. We deposited HgCdTe(100) layers on the substrates at the same time to prevent unintentional differences in the run affecting the dislocation profiles. We grew the HgCdTe(111)B layers on full 3 inch substrates in another growth run because the optimum growth conditions, such as Hg partial pressure, differ from those for HgCdTe(100) growth. The HgCdTe growth

rate was 2.5 μm/h.

We evaluated the HgCdTe layers dislocation density from the defect etch-pit density (EPD)[17] by step-etching the samples. We determined the HgCdTe layers thicknesses by controlling the step-etching rate with a bromine (Br) methanol solution. The $Hg_{1-x}Cd_xTe$ layer composition (x-value) which we determined by room-temperature infrared transmission was x = 0.20 to 0.25.

RESULTS

EPD Profiles in HgCdTe (100) and (111)B

The HgCdTe(111)B layer's EPD remained almost constant except near the HgCdTe/CdTe interface where misfit dislocations were generated (Fig. 1). This profile is similar to that in HgCdTe(111)B layers grown by LPE[17] but the EPD values are higher due to the large lattice mismatch at the CdTe/GaAs interface. In contrast, dislocations spread into the HgCdTe(100) layer and the EPD gradually decreases. The EPD values in the HgCdTe(100) layer were higher than those in the HgCdTe(111)B layer when the CdTe buffer thicknesses were the same (4 to 5 μm). The dislocation profiles in the CdTe buffer layers are probably similar to those in the HgCdTe layers for both (100) and (111)B orientations.

The difference in the EPD profiles is due to the different angles between the intertaces and the slip planes where dislocation lines are most easily generated (Fig. 2). In CdTe and HgCdTe, the {111} planes are the slip planes. The interfaces in (111)B layers are parallel to the (111) slip planes and most misfit dislocations from the interfaces propagate along the slip plane through the epitaxial layers. Since dislocation lines terminate at the side of epitaxial layers, the high EPD values in (111)B layers near the interfaces decrease rapidly. In contrast, misfit dislocations generated at the interfaces in (100) layers propagate monotonically to the growth surface because the {111} slip planes are not parallel to the (100) interfaces. The dislocation density in (100) layers decreaes gradually as dislocation lines approach each other and make dislocation loops that incorporate dislocations.

Dependence of EPD on (100) Layer Thickness

We measured the EPD profiles in the HgCdTe(100) layers with three different buffer thicknesses (Fig. 3). Each HgCdTe(100) layer's EPD decreased as the HgCdTe layer thickiness increased, although the rate of decrease was very slow in the region more than 10 μm from the HgCdTe/CdTe interface. The minimum EPD value, obtained by increasing the HgCdTe layer thickness, was governed by the CdTe buffer layer thickness. Although the EPD in HgCdTe with a 4 μm buffer reached 3 to 5×10^6 cm^{-2}, we obtained an EPD below 2×10^6 cm^{-2} for an 8 μm buffer. Most residual dislocations in the HgCdTe(100) layers were, therefore, threading dislocations from the butfer layers. Misfit dislocations generated at the HgCdTe/CdTe interface did not significantly affect the dislocation density away from the interface.

We plotted the dependence of the HgCdTe(100) layer's EPD on the thickness of the CdTe(100) buffer layers (Fig. 4). The HgCdTe layer's EPD decreased with increasing CdTe buffer thickness; however, the EPD of the layers with 8 μm and with 18 μm thick buffers were almost the same. This suggests that the dislocation density in the CdTe(100) buffer layers did not decrease in the region more than 8 μm from the CdTe/GaAs interface. This is similar to the relationship between the EPD and the HgCdTe(100) thickness.

By growing both HgCdTe and CdTe layers more than 8 μm thick, we obtained a reproducible EPD value of 1 to 3×10^6 cm^{-2} (Table I). This is comparable to the dislocation reduction which Shin et al. achieved in MOCVD-grown HgCdTe(100) layers using thermal cycle annealing.[24] To our knowledge, our best value of

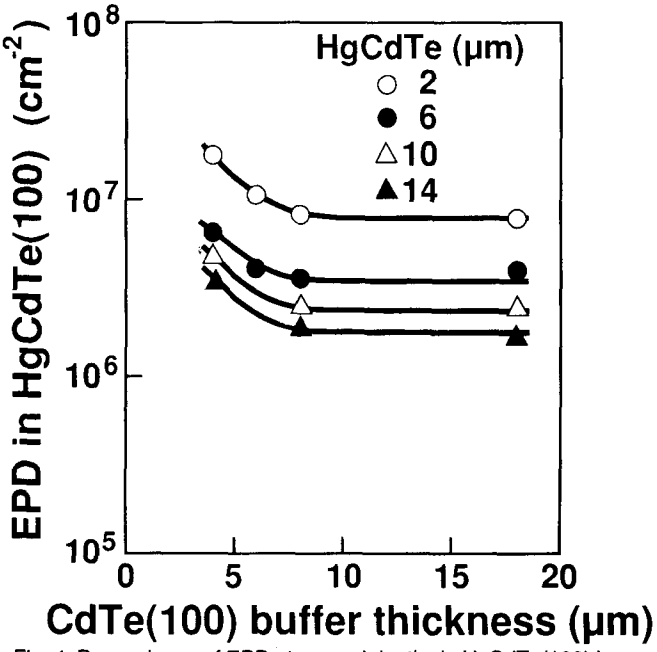

Fig. 4. Dependence of EPD at several depths in HgCdTe(100) layers on CdTe(100) buffer layers.

Table I. Reproducibility of Low-EPD HgCdTe(100) Layers with HgCdTe and CdTe Buffer Thicknesses Greater than 8 μm

Layer Index	Thickness (μm) CdTe	Thickness (μm) HgCdTe	EPD × 10^6 (cm^{-2})
101	9	10	2.1
102	8	8	3.4
103A	9	12	1.7
103B	18	12	1.5
104A	8	16	0.9
104B	18	16	0.9
201	8	12	3.0
305	8	13	2.4
307	8	13	2.2

Note: We prepared layers 103A,B and 104A,B in the same HgCdTe growth runs. We grew layers 201 and 307 on full 3 inch wafers.

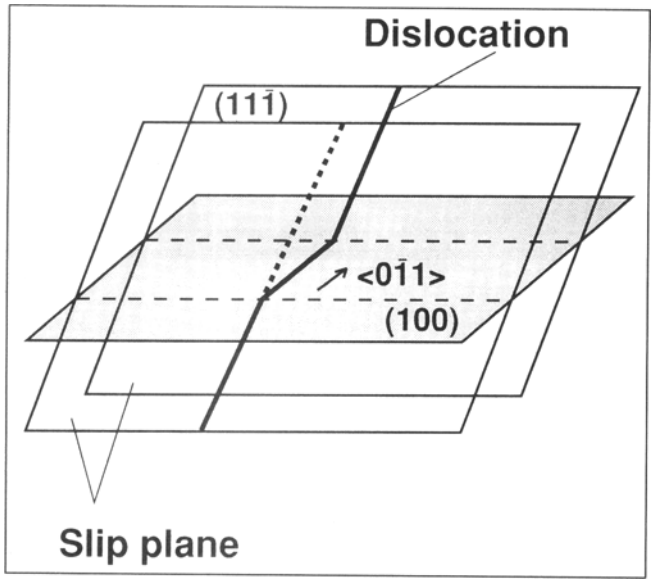

Fig. 5. Dislocation gliding in epitaxial layers.

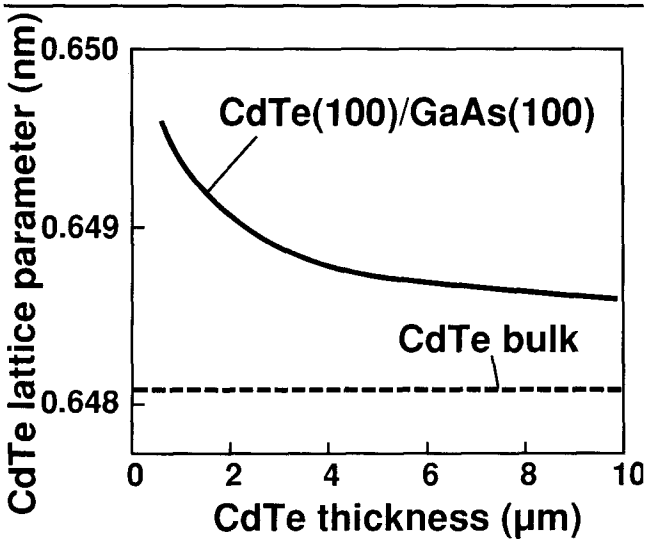

Fig. 6. CdTe lattice parameter calculated for CdTe(100)/GaAs(100). Lattice parameter is determined in the <100> direction, perpendicular to interface, and decreases with increasing CdTe thickness.

9.2×10^5 cm^{-2} is the lowest EPD reported to date for as-grown HgCdTe layers on GaAs substrates.

DISCUSSION

We think that dislocation lines on slip planes glide along the [011] direction in the epitaxial layers (Fig. 5), because the residual strain caused by the lattice mismatch at each interface acts as the dislocation motive force. This gliding increases the probability of the dislocation incorporation.

To explain the saturation of the EPD reduction with increasing layer thickness, we estimated the lattice distortion and mismatch strain. We plotted the dependence of the lattice parameter calculated[25,26] for CdTe(100)/GaAs(100) on the CdTe layer thickness (Fig. 6). The lattice parameter is defined as a value perpendicular to the interface. For the calculation, we assumed that the difference in length between the seven lattices of CdTe and the eight lattices of GaAs caused the compressive strain. The lattice mismatch strain is proportional to the difference between the calculated and measured bulk lattice parameters and the large strain (3×10^{-3} dyn) near the interface decreases to a steady value (4×10^{-4} dyn) away from the interface.

To accommodate CdTe lattice distortion, dislocations move and are incorporated more frequently near the interface where the lattice parameter's rate of change is fast. The speed of movement depends on the change in strain. Far from the interface, however, the probability of incorporation is small because dislocations do not move when the lattice distortion and strain are almost uniform. The dislocation reduction, therefore, saturates with increasing layer thickness.

CONCLUSION

We studied the EPD profiles in HgCdTe(100) layers grown by MOCVD (DAG) on GaAs(100) substrates. We compared the profiles to those in HgCdTe(111)B layers, and measured the profiles' dependence on the HgCdTe(100) and CdTe(100) buffer thicknesses. Unlike dislocations in (111)B layers, dislocations in (100) layers propagate in the growth direction due to the difference in the angles between the interfaces and slip planes. The EPD in HgCdTe(100) decreases gradually as the thicknesses of the HgCdTe and the CdTe buffer layers increase; however, the EPD reduction proceeds only in a limited area within 10 μm of each interface. The dislocation reduction mechanism we propose is that the lattice mismatch strain at each interface enhances the incorporation of dislocations. Using this model, we can explain the saturation of EPD reduction by considering the lattice distortion and mismatch strain. We obtained an EPD of 1 to 3×10^6 cm^{-2}, which is the lowest reported value for HgCdTe(100) on GaAs(100) to our knowledge.

It is possible to grow low-EPD HgCdTe(100) layers on large-area substrates. This will contribute to the development of large-scale long-wavelength infrared focal plane arrays.

ACKNOWLEDGMENTS

We thank Mr. I. Sugiyama for his useful advice and help with the calculations. We also thank Dr. H. Ishizaki for his encouragement.

REFERENCES

1. J.B. Mullin and S.J.C. Irvine, *J. Phys. D: Appl. Phys.* 14, 149 (1981).
2. S.K. Ghandhi, I.B. Bhat and N.R. Tasker, *J. Appl. Phys.* 59, 2253 (1986).
3. S.J.C. Irvine, J. Tunnicliffe and J.B. Mullin, *Mater. Lett.* 2, 305 (1984).
4. J. Tunnicliffe, S.J.C. Irvine, O.D. Dosser and J.B. Mullin, *J. Cryst. Growth* 68, 245 (1984).
5. S.K. Ghandhi, I.B. Bhat and H. Fardi, *Appl. Phys. Lett.* 52, 392 (1988).
6. D.D. Edwall, J. Bajaj and E.R. Gertner, *J. Vac. Sci. Technol.* A8, 1045 (1990).
7. S. Murakami, Y, Sakachi, H. Nishino, T. Saito, K. Shinohara and H. Takigawa, *J. Vac. Sci. Technol.* B10, 1380 (1992).

8. D.D. Edwall, *J. Electron. Mater.* 22, 847 (1993).
9. W.E. Hoke, P.J. Lemonias and R. Traczewki, *Appl. Phys. Lett.* 44, 1046 (1984).
10. H.A. Mar, K.T. Chee and N. Salansky, *Appl. Phys. Lett.* 44, 237 (1984).
11. R. Korenstein, P. Hallock, B. MacLeod, W. Hoke and S. Oguz, *J. Appl. Phys.* 62, 4929 (1987).
12. J. Elliott and V.G. Kreismanis, *J. Vac. Sci. Technol.* B 10, 1429 (1992).
13. C.D. Maxey, P. Capper, P.A.C. Whiffin, B.C. Easton, I. Gale, J.B. Clegg and A. Harker, *Mater. Lett.* 8, 385 (1989).
14. S.K. Ghandhi, N.R. Taslier, K.K. Parat and I.B. Bhat, *Appl. Phys. Lett.* 57, 252 (1990).
15. R. Korenstein, P. Hallock, B. MacLeod, W. Hoke and S. Oguz, *J. Vac. Sci. Technol.* A8, 1039 (1990).
16. S.M. Johnson, D.R. Rhiger, J.P. Rosbeck, J.M. Peterson, S.M. Taylor and M.E. Boyd, *J. Vac. Sci. Technol.* B10, 1499 (1992).
17. M. Yoshikawa, K. Maruyama, T. Saito, T. Maekawa and H. Takigawa, *J. Vac. Sci. Technol.* A5, 3052 (1987).
18. H. Takigawa, M. Yoshikawa and T. Maekawa, *J. Cryst. Growth* 86, 446 (1988).
19. H. Takigawa, *Ext. Abs. 1992 U.S. Workshop on the Physics and Chemistry of Mercury Cadmium Telluride and Other IR Materials,* (1992), p. 111.
20. R.D. Feldman, R.F. Austin, D.W. Kisker, K.S. Jeffers and P.M. Bridenbaugh, *Appl. Phys. Lett.* 48, 248 (1986).
21. R. Srinivasa, M.B. Panish and H. Temkin, *Appl. Phys. Lett.* 50, 1441 (1987).
22. H. Takigawa, H. Nishino, T. Saito, S. Murakami and K. Shinohara, *J. Cryst. Growth* 117, 28 (1992).
23. P.L. Anderson, *J. Vac. Sci. Technol.* A4, 2162 (1986).
24. S.H. Shin, J.M. Arias, D.D. Edwall, M. Zandian, J.G. Pasko and R.E. DeWames, *J. Vac. Sci. Technol.* B10, 1492 (1992).
25. Z. Feng and H. Liu, *J. Appl. Phys.* 54, 83 (1983).
26. S.N.G. Chu, A.T. Macrander, K.E. Strege and W.D. Johnston, Jr., *J. Appl. Phys.* 57, 249 (1985).